Accuracy Evaluation and Comparison of Mobile Laser Scanning and Mobile Photogrammetry Data

Accuracy Evaluation and Comparison of Mobile Laser Scanning and Mobile Photogrammetry Data

Petr Kalvoda [1], Jakub Nosek [1], Michal Kuruc [1], Tomas Volarik [1], Petra Kalvodova [1]

[1] Brno University of Technology, Veveří 331/95, Brno, Czech Republic

kuruc.m@fce.vutbr.cz

Abstract. Mobile mapping systems (MMS) are becoming used in standard geodetic tasks more common in the last years. This paper deals with the accuracy evaluation of two types of data acquired by MMS RIEGL VMX-450, and their comparison. The first type is data from mobile laser scanning (MLS). The second type is mobile photogrammetry data. The new high accurate test point field was built in area of Advanced Materials, Structures and Technologies (AdMaS) research centre that is part of Brno University of Technology. Geodetic network and test point field were measured by Trimble R8s GNSS system and Trimble S8 HP total station. The estimate of the 3D standard deviation determined by an adjustment is 2 mm. The accuracy of MLS and mobile photogrammetry data was tested based on the differences between the coordinates of the points determined from the MMS data and determined by before mentioned high precise measurement. The resulting coordinates from photogrammetric data were determined by manual detection of targets in the images. The estimate of the 3D standard deviation is 0.017 m from the MLS data, and 0.061 m from the mobile photogrammetry data. As we supposed, the mobile laser scanning data are significantly more accurate than mobile photogrammetry data. Achieved accuracy of MLS exceeds the original expectations with respect to the GNSS/IMU positioning accuracy, which is according to the manufacturer RIEGL between 0.02–0.05 m. The same scene is often scanned with multiple scanning passes to ensure high quality of the scanned point cloud, therefore we tested the relative accuracy of mobile laser scanning data from two MMS vehicle passes in the same locality of interest. Two different data sets were evaluated, first data set contains points on roads, second data set on buildings. The standard deviation estimate does not exceed 0.008 m and the maximum absolute deviation does not exceed 0.030 m for both data sets. The difference between the two passes is not significant in comparison with the accuracy criteria required for standard mapping purposes. We also compared automatic point cloud production from photogrammetry data processed in Bentley ContextCapture to the point cloud from laser scanning. The MLS data has been used as a reference because it is significantly more accurate as mentioned before. This comparison was done only on the second data set (buildings). The standard deviation estimate is 0.16 m and the maximum absolute deviation is 0.25 m. Our evaluation contains also statistical testing of outliers and stragglers. In contrast to many authors, we don't use the simplified approach 3σ rule, and in 1D. We use more exact approach using critical values of the statistics for significance levels $\alpha = 5\ \%$ and $\alpha = 1\ \%$ to stragglers and outliers test in 3D.

1. Introduction

Mobile methods become widely used to capture spatial data for many applications, for example, civil engineering, road-surveying, and 3D city modeling [1, 2]. The geometric accuracy of final products is one of the key properties, depends on a large number of factors. Accuracy can be assessed according to several criteria. Simply put, the accuracy of the final product (3D model) depends on the input data accuracy, density (resolution), and on the algorithms used.

In the case of mobile laser scanning (MLS), the input data for modeling consists of registered and filtered point clouds. The basic prerequisites for the accuracy of the 3D model are therefore the accuracy and density of MLS point clouds. This accuracy can be divided into absolute and relative components, which correspond to the positioning subsystem and mapping subsystem of MMS. The positioning subsystem uses a Global Navigation Satellite System (GNSS), Inertial Measuring Unit (IMU), and Distance Measurement Indicators (DMIs) [3, 4]. The result of GNSS, IMU, and DMI data combination in a Kalman filter is Smoothed Best Estimated Trajectory (SBET). The accuracy of SBET can be improved by using control points [5]. The mapping subsystem performs the spatial data acquisition and typically consists of one or more LIDAR sensors and cameras. Accurate calibration of both subsystems is a prerequisite for accurate georeferenced images and LIDAR data.

In the case of mobile photogrammetry, the resulting 3D model can be created in two ways: manual and automatic model generation. In the case of manual model generation, the model elements are created directly above the images. The fundamental elements are points and the final accuracy depends on their accuracy. The automatic method consists of the point cloud generation using a matching algorithm [6] and 3D model creation from this point cloud (meshing). The accuracy and density of the point cloud is the basic prerequisite for the accuracy of the 3D model.

2. MMS description

The used MMS RIEGL VMX-450 (table 1, figure 1) integrates two RIEGL VQ-450 laser scanners, modular VMX-450-CS6 camera system with four industrial cameras, POINT GREY ladybug5 spherical camera imaging system, GNSS/IMU navigation hardware, distance measurement unit VMX-450-DMI and a portable control unit VMX-450-CU.

Table 1. RIEGL VMX-450 technical characteristics [7].

Sensor	Property name	Property value
VQ-450	Measuring principle	Time of Flight
	Max. measurement rate	1.1 MHz (2×0.55 MHz), $\rho \geq 10$ % up to 140 m
	Scan rate (selectable)	up to 400 lines/sec
	Accuracy	8 mm, 1σ @ 50 m range
	Precision	5 mm, 1σ @ 50 m range
IMU/GNSS	Absolute position accuracy	0.02–0.05 m, 1σ
	Roll and pitch accuracy	0.005°, 1σ
	Yaw (heading) accuracy	0.015°, 1σ
VMX-450-CS6	Resolution	5 Mpx
	Pixel size	3.45 μm
	Sensor size	2452 × 2056 px
	Nominal focal length	5 mm
Ladybug5	Resolution	30 Mpx (5 Mpx × 6 sensors)
	Pixel size	3.45 μm
	Sensor size	2048 × 2448 px
	Nominal focal length	4.4 mm

RIEGL defines the accuracy in datasheet [7] as a degree of conformity of measured quantity to its true value in the VQ-450 section of table 1. The precision RIEGL defines in datasheet [7] as repeatability (the degree to which further measurements show the same result). Values in the IMU/GNSS section of table 1 are valid if the following conditions are fulfilled: no GNSS outages, DMI option, and post-processed using base station data. The camera calibration parameters are provided by the manufacturer. Exterior orientation parameters (positions and rotations of the cameras) can be computed by RIEGL software in post-processing. The camera data (digital camera images) can be exported in JPEG format. Optionally, index files containing a timestamp, position, and orientation can also be created for each image. The images can be exported undistorted (radial and tangential distortions are removed) [8].

Figure 1. RIEGL VMX-450 configuration

3. Test point field

Our testing is based on the analysis of the differences between the coordinates of the points determined from the MMS data and determined by a significantly more accurate method. Identifiability of these points is an important property for resulting accuracy. We can distinguish two types of point identifiability for our purposes: point identifiability in real-world and point identifiability in captured data (point clouds, images). Resulting point coordinates error consists of the identification error and the error of the used coordinate determination method. For example, the error of a point determined by a total station is affected by a point identification error in the real world. The error of a point measured from a point cloud is affected by a point identification error in a point cloud.

In this paper, we focus on the errors of the used methods. The first step is minimizing the impact of identification errors, therefore it was decided to signal the test points by targets. The signalization by targets eliminates the error of ambiguous identifiability of some natural points. It was necessary to create a test points field that will have satisfactory accuracy characteristics for the needs of MMS accuracy testing. The count of points must be sufficient to ensure the reliability of the results. The AdMaS Research Centre complex was chosen due to the easy availability and long-term sustainability of the targets. 214 points were established in the AdMaS centre, which were signalized and stabilized using checkerboard targets. Horizontal targets (119) were marked by white color on asphalt roadways (figure 2). The vertical targets (95) were made from a black matt aluminum sheet, which was supplemented with a reflective foil (figure 2). Vertical targets were placed on buildings, vertical traffic signs, concrete pillars and other suitable vertical structures. The targets on the buildings were placed in two height levels above the ground: 2 m, 10 m.

Figure 2. Checkerboard targets

The geodetic network and the test point field were measured with high accuracy. Trimble R8s GNSS system and Trimble S8 HP total station were used. Firstly, a purpose-built geodetic network was created. Secondly, test field points were determined. The coordinates of the test field points were calculated by the geodetic network least squares adjustment with a combination of GNSS and terrestrial measurements. The European Terrestrial Reference System 89 (ETRS89) and European Terrestrial Reference Frame 2000 (ETRF2000) were used [9]. The minimum-constrained network adjustment was used for computing of geodetic network. Input data in adjustment was polar coordinates measured by the total station and coordinates of four points determined by the static GNSS method. The constrained network adjustment was used for computing of test field attached to fixed points (the geodetic network). The overall accuracy of the test field determined by adjustment can be expressed as the estimate of the 3D standard deviation $s_{X,Y,Z}$ = 2 mm.

4. MMS data acquisition and processing

MMS data were acquired by two vehicle passes (in both directions) 750 m long at a speed of 20 km/h. Laser data were acquired at a frequency of 1.1 MHz. Camera data were registered every 1.5 m. The MMS trajectory was calculated using Applanix POSPac. The results of the GNSS Post Processing Kinematic method were refined and smoothed by a forward-backward Kalman filter using IMU and DMI data.

The processing of MLS data was performed in RIEGL RiPROCESS. RiPROCESS processing consists of data conversion, point clouds generation, and trajectory adjustment. In the first stage, a point clouds were created based on the POSPac trajectory. Furthermore, control points and check points in the point cloud were manually identified. More precise trajectory was processed using the RiPRECISION module based on the correspondences between the point clouds and the control points. The resulting point cloud consists of two partial point clouds corresponding to two vehicle passes. The resulting point cloud contains more than 247,000,000 points with a density of around 4 mm. The two partial point clouds contain around 123,500,000 points with a density of around 8 mm.

The camera data (exterior orientation parameters and undistorted images) were exported by RiPROCESS. These data were processed in the Bentley ContextCapture software. A total of 3,872 images was processed. Firstly, automatic keypoint extraction, automatic tie point matching, and bundle adjustment were performed. Secondly, the control points were marked manually. Thirdly, the check points were marked manually [10]. The basic parameters of photogrammetric processing are in table 2.

Table 2. Overview of ContextCapture processing parameters.

Parameter name	Parameter value
Count of photos	3872
Count of tie points	490794
Median of tie points per photo	412
Reprojection error (RMS)	0.70 px

Filtering and cloud differences were performed in CloudCompare software v2.10. The 2.5D volume function was used to calculate cloud differences at the 5 × 5 cm grid nodes. Estimations of differences between two clouds, that were projected to the horizontal plane in case of the road sub-clouds, and to the facade plane in case of the facade sub-clouds, were performed.

5. Accuracy evaluation methodology

Test field points and point clouds were transformed into a local topocentric system East, North, Up (*E, N, U*) for easier interpretation. Control points were not used as check points to ensure independent accuracy evaluation. The coordinates of points determined by geodetic method are significantly more accurate then coordinates determined from MMS data. Therefore, we can deal with coordinates E_i, N_i, U_i determined by a geodetic method as true values and deal with differences (δE, δN, δU) on check points as true errors:

$$\delta_{E_i} = E_i - \tilde{E}_i,\ \delta_{N_i} = N_i - \tilde{N}_i,\ \delta_{U_i} = U_i - \tilde{U}_i\ , \tag{1}$$

where $\tilde{E}_i$, $\tilde{N}_i$, $\tilde{U}_i$ denote coordinates determined from MMS data. If we compare pairs of the same accuracy, we have to work with the half values of the differences. The 3D differences are computed as:

$$\delta_{3D_i} = \sqrt{\delta_{E_i}^2 + \delta_{N_i}^2 + \delta_{U_i}^2}\ . \tag{2}$$

The standard deviations are estimated as:

$$s_E = \sqrt{\frac{\sum_{i=1}^{n} \delta_{E_i}}{n}},\ \ s_N = \sqrt{\frac{\sum_{i=1}^{n} \delta_{N_i}}{n}},\ \ s_U = \sqrt{\frac{\sum_{i=1}^{n} \delta_{U_i}}{n}}, s_{3D} = \sqrt{\frac{\sum_{i=1}^{n} \delta_{3D_i}}{n}}, \tag{3}$$

where n is count of differences (count of check points). Surfaces of constant probability density correspond to the errors (δ_E, δ_N, δ_U) for which:

$$[\delta_E\ \delta_N\ \delta_U]\ C_x^{-1}\ [\delta_E\ \delta_N\ \delta_U]^T = t^2, \tag{4}$$

where C_x is 3 × 3 variance-covariance matrix, and t is a size parameter [11]. The confidence ellipsoid can be expressed as:

$$\frac{\delta_E^2}{s_E^2} + \frac{\delta_N^2}{s_N^2} + \frac{\delta_U^2}{s_U^2} = t^2, \tag{5}$$

The semi-principal axes a, b, and c of the confidence ellipsoid can be expressed as $a = t \cdot s_E$, $b = t \cdot s_N$, $c = t \cdot s_U$. The error distribution probability depends on the size parameter t. The volume of the ellipsoid equals confidence level $1 - \alpha$. By changing t in equations (4), and (5), the volume and with it the confidence level is changed. For $t = 1$ the ellipsoid is called the standard confidence ellipsoid. The confidence level for this ellipsoid is $1 - \alpha = 19.1\ \%$. The probability that the error will lie inside this ellipsoid is 19.1 % [11].

An important indicator of accuracy is the occurrence of gross errors (outliers). The statistical methods of results analysis described in ISO 5725-2 [12] standard can be used. If the test statistic in "numerical outlier test" are less than or equal to its 5% critical value ($\alpha = 5\ \%$), the item tested is accepted as correct. If the test statistic is greater than its 5% critical value ($\alpha = 5\ \%$) and less than or equal to its 1% critical value ($\alpha = 1\ \%$), the item tested is called a straggler. If the test statistic is greater than its 1% critical value ($\alpha = 1\ \%$), the item is called a statistical outlier [12].

The size parameter of confidence ellipsoid for $1 - \alpha = 95\ \%$ probability that the error lie inside the ellipsoid is $t = 2.8$, and for $1 - \alpha = 99\ \%$ probability is $t = 3.4$. The points with errors ($\delta_E, \delta_N, \delta_U$) that lie inside 95% confidence ellipsoid ($Z_{95\%}$) are accepted. The points with errors ($\delta_E, \delta_N, \delta_U$) that lie outside 95% confidence ellipsoid ($Z_{95\%}$) and inside or on 99% confidence ellipsoid ($Z_{99\%}$) are called stragglers. The points with errors ($\delta_E, \delta_N, \delta_U$) that lie outside 99% confidence ellipsoid ($Z_{99\%}$) are called outliers.

This test can be simplified using the confidence sphere instead of the ellipsoid. The 3D errors that meet the condition $\delta_{3D} \leq 2.8 \cdot s_{3D}$ are accepted. The 3D errors that meet the condition $2.8 \cdot s_{3D} < \delta_{3D} \leq 3.4 \cdot s_{3D}$ are called stragglers. The 3D errors that meet the condition $\delta_{3D} \geq 3.4 \cdot s_{3D}$ are called outliers.

6. Results

The accuracy of MLS and mobile photogrammetry data was tested based on the differences between the coordinates of the points determined from the MMS data and determined by before mentioned high precise measurement. The resulting coordinates from photogrammetric data were determined by manual detection of targets in the images. The overview of control points and check points location is shown in figure 3. The results of the accuracy evaluation at check points are described in table 3.

The results of the relative accuracy evaluation from two MMS vehicle passes are described in table 4. Two different MLS data sets were evaluated, the first data set contains points on roads (see column 2 in table 4 and figure 4), the second data set on the facade (see column 3 in table 4 and figure 5 left). We also compared automatic point cloud production from photogrammetry data processed in Bentley ContextCapture to the point cloud from laser scanning. The MLS data has been used as a reference because it is significantly more accurate as mentioned before. This comparison was done only on the second data set on the facade (see column 4 in table 4 and figure 5 right). These analyses are based on the differences in the point clouds computed in CloudCompare v2.10.

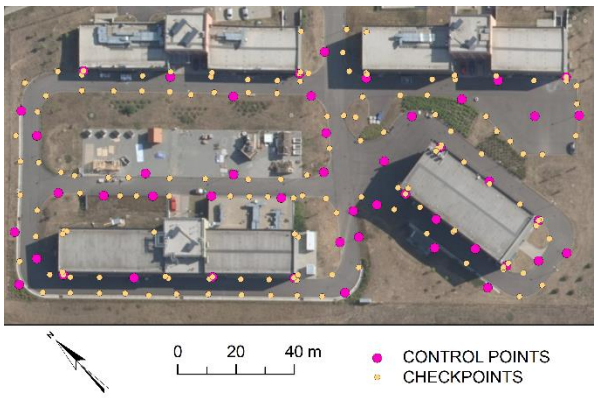

Figure 3. Overview control points and check points location

Table 3. Accuracy evaluation at check points

	MOBILE LASER SCANNING				MOBILE PHOTOGRAMMETRY			
	E	*N*	*U*	*3D*	*E*	*N*	*U*	*3D*
Count of control points	48	48	48	48	48	48	48	48
Count of check points	158	158	158	158	96	96	96	96
Maximum absolute deviation	0.037	0.025	0.044	0.050	0.095	0.216	0.124	0.230
Standard deviation	0.011	0.009	0.009	0.017	0.031	0.045	0.027	0.061

Table 4. Relative accuracy evaluation of point clouds

	Two passes MLS roads	Two passes MLS facade	MLS × photogrammetry facade
Count of grid points	83039	14510	10120
Maximum absolute deviation	0.030	0.028	0.249
Standard deviation	0.006	0.008	0.164

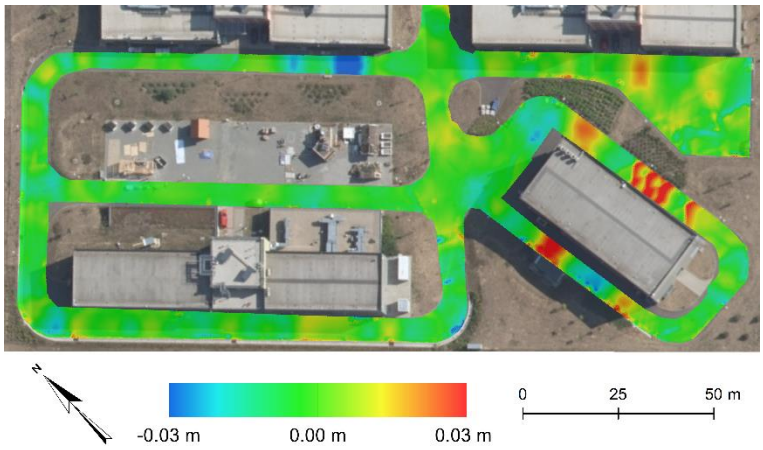

Figure 4. Visualization of the differences between the two passes of MLS – roads

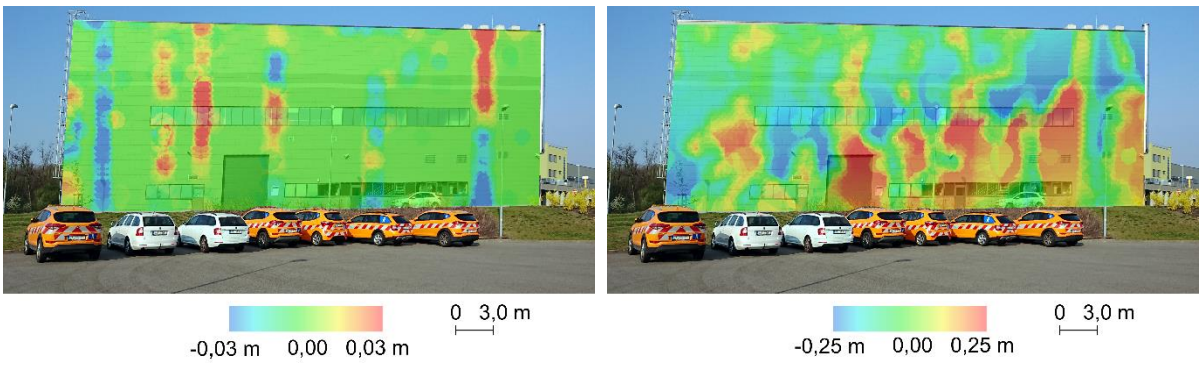

Figure 5. Visualization of the differences between the two passes of MLS on the facade (left), between MLS and mobile photogrammetry on the facade (right)

The error distribution on the check points is displayed in the histograms in figures 6, 7. The results of the 3D error test of outliers and stragglers on the check points using $Z_{95\%}$ and $Z_{99\%}$ confidence spheres are shown in table 5, and confidence ellipsoids in table 6 and figure 8.

Table 5. The results of the outliers and stragglers test on check points using confidence sphere

	MOBILE LASER SCANNING	MOBILE PHOTOGRAMMETRY
$\delta_{3D} \leq Z_{95\%}$	157	92
$Z_{95\%} < \delta_{3D} \leq Z_{99\%}$	1	2
$\delta_{3D} > Z_{99\%}$	0	2

Table 6. The results of the outliers and stragglers test on check points using confidence ellipsoids

	MOBILE LASER SCANNING	MOBILE PHOTOGRAMMETRY
$(\delta_E, \delta_N, \delta_U) \leq Z_{95\%}$	142	88
$Z_{95\%} < (\delta_E, \delta_N, \delta_U) \leq Z_{99\%}$	13	4
$(\delta_E, \delta_N, \delta_U) > Z_{99\%}$	3	4

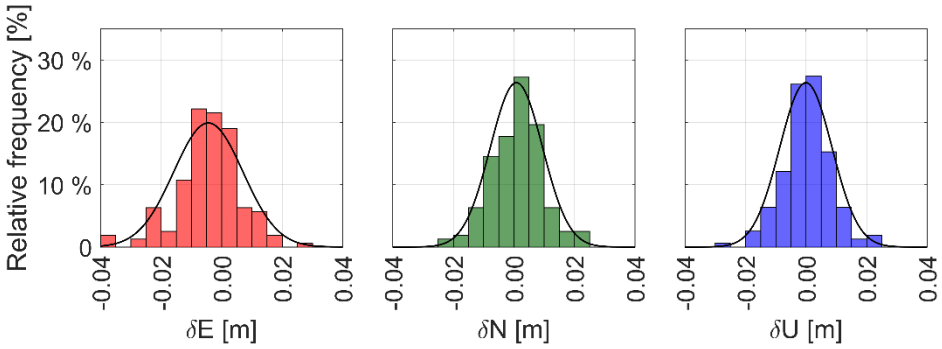

Figure 6. Histograms of mobile laser scanning errors on check points

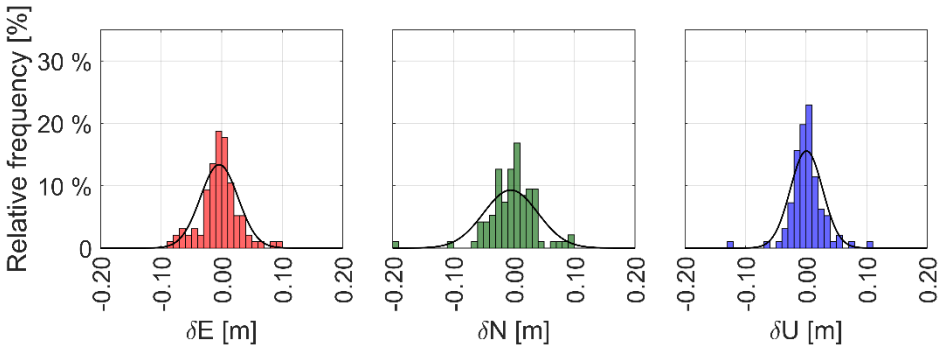

Figure 7. Histograms of mobile photogrammetry errors on check points

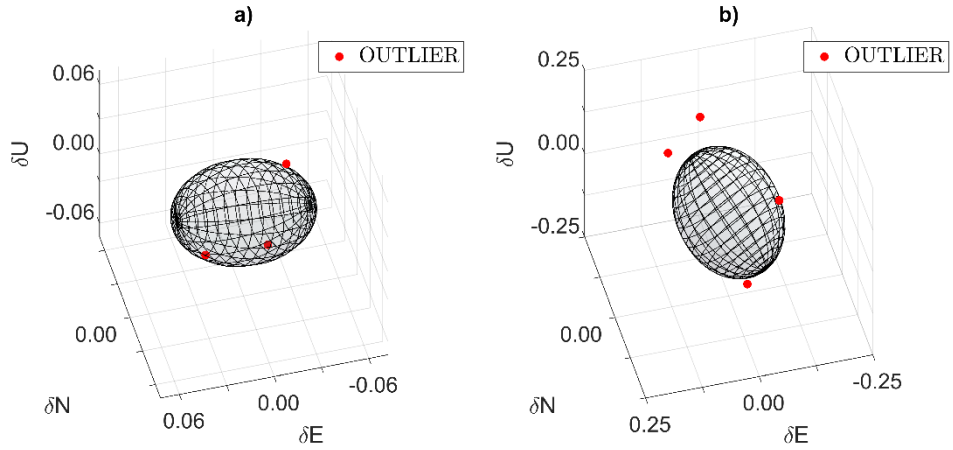

Figure 8. Confidence ellipsoids of mobile laser scanning (left) and mobile photogrammetry (right)

7. Conclusions

The accuracy evaluation and comparison of MLS and mobile photogrammetry data acquired by MMS RIEGL VMX-450 have been performed. The new high accurate test point field was built, the estimate of 3D standard deviation value is 2 mm. The accuracy evaluation of MMS data using this point field was done independently for MLS and mobile photogrammetry. The accuracy of the MLS is characterized by the estimate of the 3D standard deviation, that value is 0.017 m, and by maximum absolute 3D deviation, that value is 0.050 m. The achieved accuracy is better than the GNSS/IMU positioning uncertainty quoted by the MMS manufacturer RIEGL (0.02–0.05 m, 1σ) and also than results presented in [4] for high-end MMS. This is probably achieved by the trajectory improvement using the control points. The accuracy of mobile photogrammetry is characterized by the estimate of the 3D standard deviation, that value is 0.061 m, and by maximum absolute 3D deviation, that value is 0.23 m. As we supposed, the mobile laser scanning data are significantly more accurate than mobile photogrammetry data.

The relative accuracy evaluation from two MMS vehicle passes on two different MLS data sets was performed. The first data set contains points on roads, the second data set on the facade. The relative accuracy of road data set is characterized by the estimate of the 3D standard deviation, that value is 0.006 m, and by maximum absolute 3D deviation, that value is 0.030 m. The relative accuracy of facade data set is characterized by the estimate of the 3D standard deviation, that value is 0.008 m, and by maximum absolute 3D deviation, that value is 0.028 m. The difference between the two passes is not significant in comparison with the accuracy criteria required for standard mapping purposes. These results are consistent with the uncertainty quoted by the MMS manufacturer RIEGL (8 mm, 1σ) and with results presented in [13].

The relative accuracy evaluation of the mobile photogrammetry point cloud was evaluated on facade using MLS point cloud as reference. The standard deviation estimate is 0.16 m and the maximum absolute deviation is 0.25 m. The accuracy of the mobile photogrammetry point cloud is significantly lower than photogrammetric data determined by manual detection of targets in the images, as we supposed. This test quantified the ratio of the resulting accuracies.

The relative number of outliers based on the $Z_{99\%}$ confidence ellipsoid 3D error test is 2.1 % of the tested points total number in the case of MLS and 4.5 % in the case of mobile photogrammetry. The relative number of outliers based on the $Z_{99\%}$ confidence sphere 3D error test is 0.0 % of the tested points total number in the case of MLS and 2.2 % in the case of mobile photogrammetry. The relative number of outliers is acceptable for standard mapping purposes.

Future work will focus on testing the influence of the count of control points on the accuracy of resulting 3D data. We will also focus on the analysis of the influence of trajectory accuracy on the local accuracy of 3D data.

Acknowledgment
This paper was supported by faculty research project FAST-S-19-5704 "Geometric accuracy of mobile mapping systems" of internal grant system BUT.

References

[1] O. Al-Bayari, "Mobile mapping systems in civil engineering projects (case studies)," *Applied Geomatics 11*, pp. 1–13, 2019.
[2] G. R. Kimpton, M. Horne, D. Heslop, "Terrestrial Laser Scanning and 3D Imaging: Heritage case study – The Black Gate, Newcastle upon Tyne," *International archives of photogrammetry, Remote sensing and spatial information sciences,* vol. XXXVIII, Part 5, commission V symposium, pp. 325–330, 2010.
[3] I. Puente, H. González-Jorge, J. Martínez-Sánchez, P. Arias, "Review of mobile mapping and surveying technologies," *Measurement*, vol. 46, Issue 7, pp. 2127–2145, 2013.
[4] L. Mattheuwsen, M. Bassier, and M. Vergauwen, "Theoretical accuracy prediction and validation of low-end and high-end mobile mapping system in urban, residential and rural areas, Int. Arch. Photogramm," *ISPRS - International Archives of the Photogrammetry, Remote Sensing and Spatial Information Sciences*, XLII-2/W18, pp. 121–128, 2019.
[5] A. P. Kerstinga, P. Friess, "Post-mission quality assurance procedure for survey-grade mobile mapping systems," *The International Archives of the Photogrammetry, Remote Sensing and Spatial Information Sciences*, vol. XLI-B1, pp. 647–652, 2016.
[6] T. Luhmann, S. Robson, S. Kyle, J. Boehm, "Close-range photogrammetry and 3D imaging," 3rd edition, 2020.
[7] Riegl Laser Measurement Systems GmBH, "RIEGL VMX-450, Compact Mobile Laser System, Data Sheet," 2015.
[8] Riegl Laser Measurement Systems GmBH, RiPROCESS user guide, Austria, 2016.
[9] Z. Altamimi, "EUREF Technical Note 1: Relationship and Transformation between the International and the European Terrestrial Reference Systems," 2018.
[10] Bentley Systems, "ContextCapture User Guide," 2019.
[11] P. Cederholm, "Deformation analysis using confidence ellipsoids," *Survey Review*, United Kingdom, 37:287, pp. 31–45, 2003.
[12] International standard ISO 5725-2:1994 Accuracy (trueness and precision) of measurement methods and results – Part 2: Basic method for the determination of repeatability and reproducibility of a standard measurement method, 1994.
[13] I. Toschi, P. Rodríguez-Gonzálvez, F. Remondino, S. Minto, S. Orlandini, and A. Fuller, "Accuracy evaluation of a mobile mapping system with advanced statistical methods," *ISPRS - International Archives of the Photogrammetry, Remote Sensing and Spatial Information Sciences,* vol. XL-5/W4, pp. 245–253, 2015.